Multiscale study of poly(butylene terephthalate) hydrolysis

C. Loyer[a,b], G. Régnier[a], V. Duval[b], E. Richaud[a,*]

[a] Laboratoire PIMM, Arts et Métiers Institute of Technology, CNRS, Cnam, HESAM Université, 151 boulevard de l'Hôpital, 75013 Paris, France
[b] APTIV, Z.I des Longs Réages, 28230 Epernon, France

A B S T R A C T

This paper reports the hydrolysis of several PBT materials (pigmented or not). Degradation was monitored by gel permeation chromatography (chain scission), DSC (crystalline morphology), tensile test (residual mechanical properties) and DVS (polymer-water interaction). The embrittlement comes from chain scission associated with a small chemicrystallization effect. Results lead to the proposal of a kinetic model for the chain scission rate aimed to describe the auto-acceleration effect induced by carboxylic acids (chain ends) and successfully compared to results both from this work or literature. The mixed "average molar mass – crystallinity" criterion proposed in a previous paper was specified. At last, the effect of pigments is illustrated and shows that carbon black (present in particular in one masterbatch) plays an aggravating role on hydrolysis.

1. Introduction

Embrittlement caused by chains cleavage is a well-known phenomenon for semi-crystalline polymers undergoing chemical (hydrolytic or oxidative) ageing and has been extensively investigated for polyolefins or polyamides for example [1–3]. Recently, such embrittlement criteria was highlighted for poly(butylene terephthalate) (PBT) [4]. In order to help lifetime prediction, a last step is to define degradation rate regarding ageing conditions and finally establishing a degradation modelling.

In terms of chemical mechanisms driving the embrittlement, PBT was extensively studied in the case of UV, thermolysis and thermal oxidation [5–10]. Some authors studied the effect of humidity especially on mechanical properties of filled and unfilled PBTs [11–15]. They defined an Arrhenius diagram based on a mechanical criterion [11,15]. However they did not considered the hydrolysis of PBT as an autocatalysis phenomenon so that distortions in the Arrhenius diagram are expected and would lead to significant deviations [16].

Establishing an accurate kinetic model is thus of key importance. Kelleher et al. [17] did a pioneering work where based on the exploitation of MFI. A key result is that the apparent rate of hydrolysis increases with initial MFI suggesting the role of chain ends on hydrolysis. In case of PET, Ballara and Verdu [18] have defined a kinetic model for the polymer degradation where auto-acceleration comes from the continuous increase in water solubility caused by chain scission process and the subsequent build-up of new hydrophilic functions (carboxylic acids, alcohols). However, this result can be discussed regarding the data of Kelleher et al. [17]. where difference in hydrolysis rate is visible even at very early ageing conversion degrees.

Furthermore, colored pigmented polymers stability was mainly studied in the case of polyolefins thermal [19,20] or UV light ageing [21] meanwhile, to our knowledge, pigmented PBT stability was not studied in case of hydrolysis.

Finally, the aims of the present study are thus to:

- investigate the polymer-water interaction for several PBT grades in order to highlight the microstructural effect on water uptake
- propose a kinetic model describing the auto-acceleration and the chain ends effect
- confirm the failure criteria established for one PBT grade for other PBT materials differing by their initial molar mass.
- understand the influence of hydrolysis on pigmented PBT grades used as masterbatches.

2. Experimental

2.1. Materials

5 injection grades of poly(butylene terephthalate) were used in this study (detailed in Table 1). They were processed into about 150 to 200 μm thick films with a GIBITRE compacting press (200 bar) at 230°C with an approximately 1min30 cycle (this temperature was chosen low enough to limit thermal degradation[4]).

Table 1
Initial average molecular masses (M_n, M_w) and polydispersity index PDI for films.

	M_n (kg/mol)	M_w (kg/mol)	PDI	χ_c (%)	Features
PBT1	33.8	74.7	2.1	28.2	None
PBT2	35.5	76.9	2.2	33.4	None
PBT3	29.9	63.4	2.1	36.3	Nucleating agent
PBT-CB	12.8	35.4	2.8	38.1	82.5% of PBT Carbon black pigment
PBT-G	24.9	57.1	2.3	37.9	70% of PBT green pigment

2.2. Ageing conditions

Films and plates previously prepared were immerged in distilled water in closed vessels and placed in a ventilated oven (AP60 by System Climatic Service) at 80°C. After exposure, films were dried at 120°C under vacuum for 4 hours before any testing.

The possible effect of thermal oxidation was investigated by subjecting PBT1 films in ventilated oven (AP60 by System Climatic Service) at 80°C.

2.3. Characterization

2.3.1. Tensile testing

Uniaxial tensile testing was carried out at room temperature at 10 mm/min using an INSTRON 4301 machine with a 100 N cell. No extensometer was used during tests hence only the cross head displacement was recorded. Samples were punched using a H3 hole punch with a 150-200 μm thickness (neck length $L_0 = 20$ mm and 4 mm).

2.3.2. Gel permeation chromatography

Gel Permeation chromatography (GPC) were performed by PeakExpert laboratory based on a detailed experiment in [22]. PBT samples were dissolved in Hexafluoroisopropanol (HFiP) with 0.1M potassium trifluoride (KTFA) at 2.0 g/L. The injection volume was 100 μL at 40°C. The measurement was performed using a e2695 GPC (Waters) and the detection with a RID Waters 2414 refractometer. Three columns were used: one PSS PFG 10 μm, 1000Å, ID 8,0 mm × 100 mm as a pre-column and 2 columns PSS PFG 10 μm, 1000Å, ID 8.0 mm × 300 mm. Post treatment was done by using PSS-WinGPC Unity software and was based on the integration of signals such as illustrated in [23] Molar masses were given as PMMA equivalent.

2.3.3. Differential scanning calorimetry

Morphological changes were followed with a Q1000 by TA instrument. Prior to any measurement, DSC apparatus was calibrated with an indium standard. About 6-8 mg of virgin or aged PBT sealed in standard aluminum pans were subjected to two cycles: a heating from 30°C to 250°C followed by a cooling 250°C to 0°C and the second heating from 0°C to 250°C and finally a cooling from 250°C to 0°C. Both cycles were performed at 10°C/min rate.

The crystallinity was measured from the melting peak enthalpy ΔH_f using $\Delta H_f^\circ = 140$ J/g for a 100% crystalline PBT sample [24]. For samples with carbon black, the crystallinity was determined using the following correction (for example for the presence of pigments):

$$\chi_c(\%) = 100\left(\frac{\Delta H_f}{w_{PBT}\Delta H_f^\circ}\right) \quad (1)$$

where

χ_c (%) is crystallinity, and w_{PBT} is the PBT ratio in weight percent in the sample [25]

2.3.4. Dynamic vapour sorption

Dynamic vapour sorption were performed with DVS 1000 from SMS at two temperatures, 50°C and 80°C and under three relative humidity values (30, 50 and 90%HR) with the following absorption procedure: 4 h at 0%HR, 6 h at 30%HR, 6 h at 50%HR and 6 h and 90%HR.

These parameters were checked on film only avoiding water diffusion in the sample. Before any testing, films were put at 50°C under vacuum for at least 24 h.

2.3.5. Fourier transform infrared spectroscopy

FTIR measurements were performed using a Frontier 100 device from Perkin-Elmer driven by Perkin Elmer Spectrum software. Analyses were done by accumulating 16 scans between 650 and 4000 cm^{-1} in ATR mode (with a diamond crystal).

3. Results

3.1. Water sorption (DVS data)

Fig. 1 depicts the relative mass uptake for several grades of PBT at 50 and 80°C. At low Relative Humidities (HR), curves are almost linear for pure matrices (PBT1, PBT2 and PBT3).

① For the three grades without pigment or dyes (PBT1, PBT2 and PBT3), mass uptake changes almost linearly with water activity, i.e. that water absorption follows Henry's law. The comparison of Fig. 1a and Fig. 1b suggests that there is a minor effect of temperature. It can also be easily spotted that maximal water uptake of PBT1, PBT2 and PBT3 grades are roughly identical. The values obtained here are quite in line with a previous study [12] which obtained a mass variation of about 0,8% ($\chi_c = 25.4\%$) by immersing PBT in water which could explained the slightly higher value compared to our study.

② PBT-G contains a copper phthalocyanine pigment which is in essence insoluble in PBT amorphous phase. Since water only dissolves in PBT amorphous phase, the overall water uptake in PBT Δm_{water} depends on weight fraction of crystals (χ_c) and of pigments ($w_{pigments}$):

$$\Delta m_{water} = \Delta m_{water,a}\left(1 - \chi_c - w_{pigments}\right) \quad (2)$$

According to this relation, the presence of pigments decreases the water uptake but the decrease must be low here since $w_{pigments}$ is low. On the other hand, pigment can act as nucleating agents, i.e. that even a small value of $w_{pigments}$ can induce a strong increase in χ_c and a quite lower water uptake. Here, DSC data (Table 1) and DVS ones (Fig. 1) indicate that phthalocyanine pigment only displays a minor role on water uptake despite a visible impact on crystallization temperature [26] and crystallinity.

③ In the case of PBT-CB sample, there is a significantly higher water uptake despite a crystallinity comparable with other PBT materials (Table 1). It is well established that carbon black has a quite complex surface chemistry with several hydrogen bonding groups [27] responsible of water absorption at its surface [27,28].

To better quantify and model the water sorption, we decided to extract the slope from sorption isotherms of PBT1, PBT2 and PBT3. Data are given in Table 2 and confirm that the Henry's law is almost verified since the correlation coefficient R^2 remains quite close to 0.99.

In such cases, previous studies have shown that equilibrium water absorption in linear polymer is an additive property [29,30] and can be calculate as follows:

$$H = \frac{W_m M}{100*18} = \sum^{n_i} H_i = 2H_{ester} + \frac{1}{M_n}(H_{ac} + H_{al}) \quad (3)$$

where

H is the number of water molecules in a monomer unit,

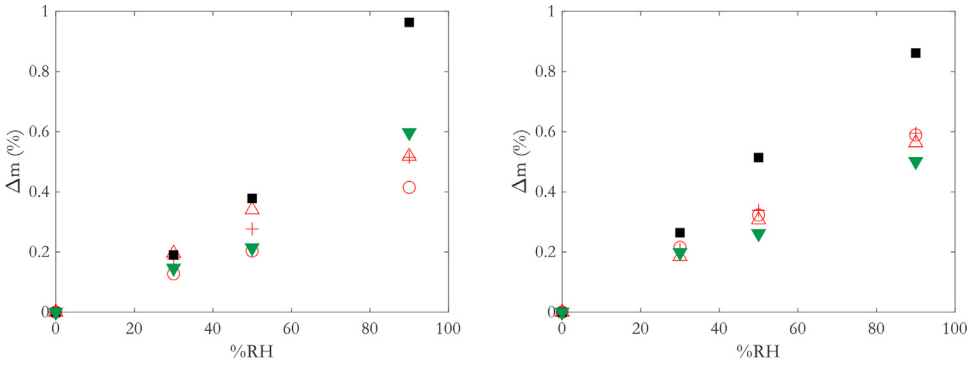

Fig. 1. Weight increase (%) at 50°C (a) and at 80°C (b) for PBT1 (+), PBT2 (○), PBT3 (△), PBT-CB (■) and PBT-G (▼).

Table 2
Henry's parameter (trend and correlation coefficient) and extrapolated H value at saturation for all tested grades.

	50°C slope	R^2	H_{max}	80°C slope	R^2	H for 100 RH% (H_{max})
PBT1	0,0057	0,9989	0.1	0,0067	0,9993	0.11
PBT2	0,0045	0,9933	0.11	0,0055	0,9979	0.11
PBT3	0,006	0,9839	0.09	0,0062	0,9998	0.13
PBT-CB	0,0097	0,9427	/	0,0097	0,9959	/
PBT-G	0,006	0,9393	/	0,0056	0,99	/

W_m the equilibrium water absorption in weight percent in the amorphous phase,

M the molecular mass of the monomer unit (g/mol),

H_i the molar contribution of the group n_i the number of groups I in the monomer unit

Considering the almost linear behavior of all virgin PBT, we calculated the H_{max} meaning the H value at 100%RH. Table 2 summarizes H_{max} values for each virgin grade at 50°C and 80°C. Values are around 0.1, consistently with other data for PBT, PET, PCL and PMMA [12,31–33] suggesting that in all cases, about 1 molecule of water is solubilized by 10 ester groups.

According to Table 2, there is only a limited effect of M_n (i.e. alcohols and acid chain ends) indicating that, in the range of PBT grades for industrial purposes, the specific absorption due to those groups is of second order and that the reported values for water sorption are quite universal.

3.2. Mechanical properties changes

Prior to any ageing, tensile tests were performed on the three materials PBT1, PBT2 and PBT3. These tests were not conducted on the colored PBTs because their initial weight molar mass (Table 1) were either lower than the M'_{wc} previously established [4] or in the transition area resulting in brittle materials.

According to Fig. 2, PBT2 and PBT3 display a lower maximal strain and elongation at break than PBT1. As the initial weight molecular mass are roughly identical for these resin one explanation could be the higher crystallinity for PBT2 and PBT3 compared to PBT1.

PBTs grades display a plasticity loss during hydrolysis ageing (Fig. 3) at 80°C. Ultimate strain is reduced by more than 50% of its initial value after about 1350 h meanwhile free standing films aged in oven the same duration at the same temperature did not display any significant change in mechanical properties. It suggests that hydrolytic ageing clearly predominates over thermal ageing. The next step is to explain those changes by the analysis of macromolecular architecture.

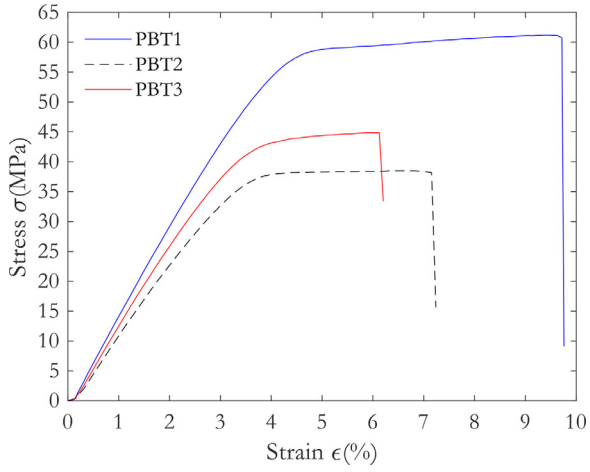

Fig. 2. Typical stress-strain curves for virgin PBTs prior hydrolysis. Errors bars are not displayed for a better clarity.

3.3. Macromolecular changes

Let us recall that intrinsic mechanical properties of semi crystalline polymers depend in great part on average molar mass and crystalline morphology.

It was previously established that hydrolysis exclusively leads to chain scissions [25,34], as it can be also deduced from Fig. 4a with the major decrease in weight molar mass M_w meanwhile under air at 80°C, M_w only dropped from 75 kg/mol to 66 kg/mol after 1350 h exposure.

The concentration in chain scission can be calculated from Saito's equation [35]:

$$\frac{1}{M_w} - \frac{1}{M_{w,0}} = \frac{s}{2} \tag{4}$$

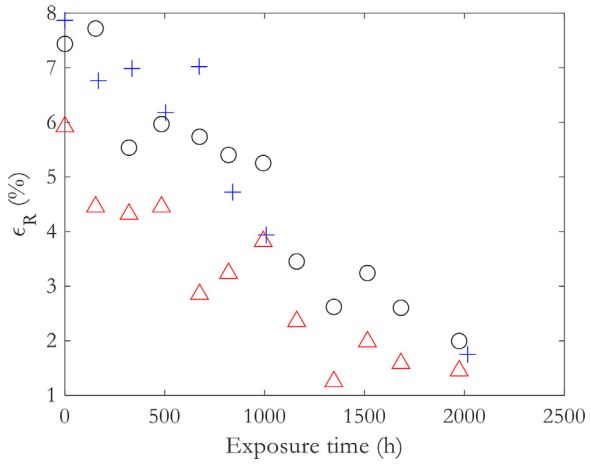

Fig. 3. Elongation at break average changes for PBT1 (+), PBT2 (○) and PBT3 (△).

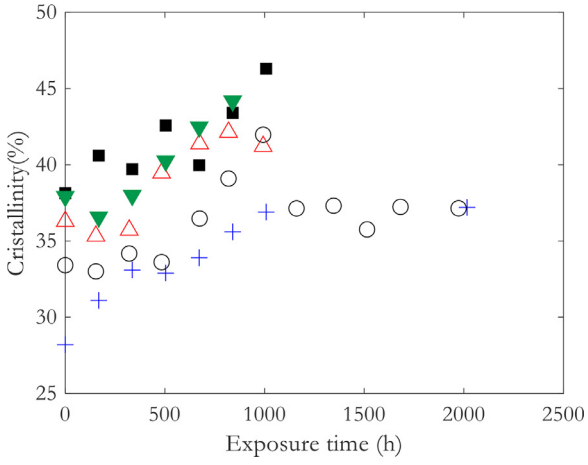

Fig. 5. Changes of crystallinity for PBT1 (+), PBT2 (○) and PBT3 (△), PBT-CB (■) and PBT-G (▼).

The concentration in chain scissions are given in Fig. 4b. The most striking results are that:

- at 80°C, degradation of immerged samples is mainly caused by hydrolytic ageing. For instance, Eq. 4 shows that samples aged in presence of water have undergone almost 10 times more chain scissions than samples aged in presence of air. In other words, even if there were some traces of oxygen in waters despite cautious degassing, the contribution of thermal oxidation to our results would be negligible, so that those phenomena will not be taken into account in the kinetic modeling part.
- the rate of chain scission is almost the same for unpigmented PBT matrices,
- reversely, it is significantly higher for pigmented matrices i.e. about 3 to 4 times for PBT-CB and twice for PBT-G. At least two reasons can be considered: the presence of pigments and/or the lower initial weight molar mass. They will be discussed later.

Another change involving mechanical properties changes is the crystallinity because of two mechanisms: the annealing and the chemicrystallization, where chain segments having undergone scissions in amorphous phase migrate into crystalline phase. Fig. 5 depicts the increase in crystallinity.

At first, the "initial" increase in crystallinity usually associated to annealing is low, suggesting this phenomenon does not occur in hydrolytic ageing. Following the results from Fig. 5, the increase rate in χ_c seems to be identical for every PBT regardless the presence of pigments. This is well confirmed by the shape of thermograms (see Supplementary data SI-1 where no signal testimony of an endotherm for PBT 1, 2, 3 is visible). Moreover, crystalline ratio value of virgin PBT grades seems to plateau after around 1000 h.

The visible endotherm on PBT-CB and PBT-G thermograms (see 'APPENDIX') around 118°C seems linked to the additives. It disappears at long ageing times. Therefore, we do not believe it is testimony of an annealing peak. Hence, we did not consider it when calculating crystallinity.

3.4. Molecular changes

FTIR-ATR measurements were also conducted to highlight possible chemical changes induced by hydrolytic degradation and thermal oxidation and conclude on the prominent mechanism.

According to Fig. 6, there is no clear molecular change for ageing in presence of air so that thermal oxidation can definitively be neglected. For water exposure, it seems that even after 6 weeks of exposure there is a certain sharpening of carbonyl peak (in link with ester disappearance) with a very slight increase of carboxylic acids (1675-1700 cm^{-1}) and carboxylate (1525-1550 cm^{-1}) signals corresponding to hydrolysis induced chain ends. It suggests that hydrolyzed chain segments can be extracted, which would need to be confirmed in the following.

4. Discussion

Based on the results presented in the previous section, we can discuss about the universality of structure properties relationships

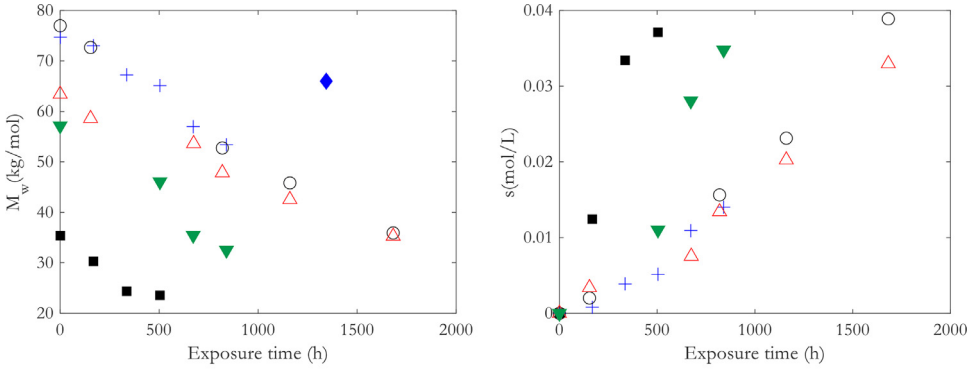

Fig. 4. Changes of weight molecular mass (a) and chain scission (b) for PBT1 (+), PBT2 (○), PBT3 (△), PBT-CB (■), PBT-G (▼), PBT1 after thermal oxidation at 80°C (♦).

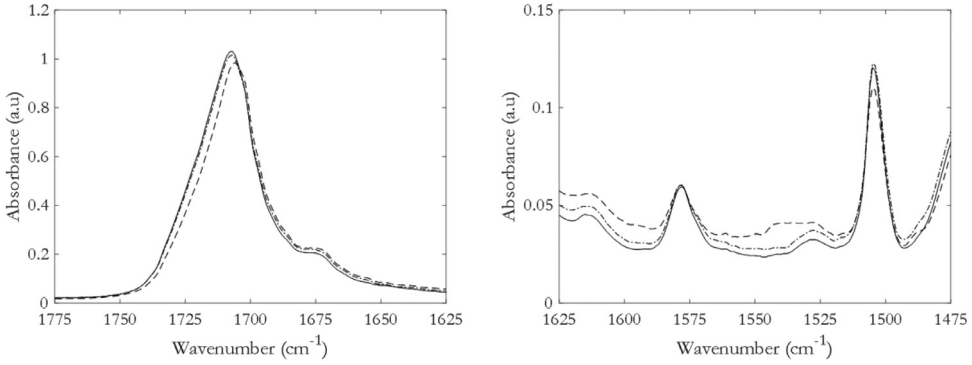

Fig. 6. FTIR-ATR Carbonyl area (a) and carboxylate area (b) of virgin PBT1 (–), PBT1 after 674 h (– –) at 80°C in water and 1350 h (– • –) under air at 80°C.

Table 3
Embrittlement molar mass M'$_{wc}$ and chemicrystallization yield (y) for each PBT grades.

	PBT1	PBT2	PBT3	PBT-CB	PBT-G
t ($\varepsilon_{R,c} = \varepsilon_{R,0}/2$)	6 weeks	7 weeks	4 weeks	-	-
M'$_{wc}$ ($\varepsilon_{R,c} = \varepsilon_{R,0}/2$)	≈ 50 kg/mol	≈ 46 kg/mol	≈ 52 kg/mol	-	-
y	33	23	19	5	10

involved induced in PBT embrittlement for several PBT grades. The second aim is to adapt a kinetic model for hydrolysis which could be working for each industrial PBT grades, with various viscosity (related to initial molar mass), or pigments.

4.1. On the embrittlement criteria during PBT hydrolysis

In our previous work, we proposed an embrittlement criterion for PBT submitted either to thermal of hydrolytic ageing but it arises the question of its "universality", i.e. if it can be adapted to other PBT grades. Here, this study allows us to precise the embrittlement criteria of PBTs undergoing chain scission during their ageing. Table 3 gives for example the molar mass of samples of each PBT grade in the domain of the "ductile to brittle transition". Values are slightly lower than in our previous study (57-65 kg.mol^{-1}).

A plausible explanation of the difference between each grade is the double origin of the embrittlement which originates from the decrease of molar mass and the increase in crystallinity, by the so called chemicrystallization mechanism [36]:

The chemicrystallization yield was determined before embrittlement using the following relation:

$$y = \frac{1}{M_m}\frac{d\chi_c}{ds} \tag{5}$$

where M_m is the monomer molar mass.

Results are summed up in Table 3. We can say that for virgin PBT the chemicrystallization yield is depending on the initial crystallinity and between the value of other common polymers as PA6 and PE [1,37]. However, the pigmented PBTs have a lower chemicrystallization yield probably due to the presence of pigment in the matrix. It is highly possible that the morphology of carbon black is equivalent as a barrier preventing from further crystallization. Besides, at the initial state the crystallinity of PBT-CB is near the maximum value observed for PBT (≈ 40%).

Those results allow precising the ductile/brittle transition area given in our previous study, and confirm its validity for several PBT grades, both for hydrolysis and thermal oxidation (Fig. 7).

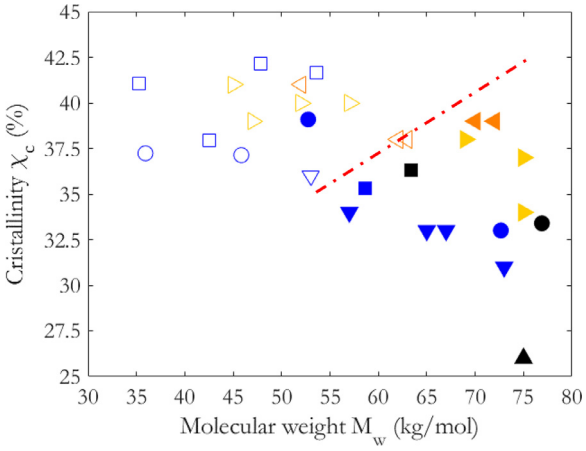

Fig. 7. Embrittlement border according to hydrolysis conditions for PBT1 (▼), PBT2 (●) and PBT3 (■). Upwards triangles (▲) represent thermal oxidation for PBT1 at 180°C (►) and 210°C (◄) [4].

4.2. Proposal of a kinetic modelling

The hydrolysis of polymers holding esters or amides was already addressed in the past for several polymers such as PA11 [38], PET [25,39], PBT [40] TPU [16] or tridimensional polyesters [41]. Several models were proposed for reversible hydrolysis where chains scission are compensated by polycondensation [38], for hydrolysis controlled by water diffusion[38], [42] or auto-accelerated hydrolysis where each hydrolysis reaction generates an acid increasing water solubility and later the hydrolysis rate (but this seems contradictory, in a first approach, with DVS data). Here, kinetic curves for chain scission display a positive concavity, which was explained as follows: the hydrolysis reaction of ester can be written as:

(a) $e + w \rightarrow ac + s(k_u)$

in its simple form, so that

$$\frac{-de}{dt} = \frac{ds}{dt} = k_u\,[e]\,[w] \tag{6}$$

However, it is known that the reaction generates a carboxylic acid which is a strong catalyst for further hydrolytic reactions. A second reaction must be added:

$$e + ac + w \rightarrow e + s(k_c)$$

Hence

$$\frac{d[e]}{dt} = -k_u[w][e] - k_c[w][e][ac] \quad (7)$$

i.e., since each ester is transformed into an acid by hydrolysis:

$$\frac{d[e]}{dt} = -k_u[w][e] - k_c[w][e]([e]_0 - [e]) \quad (8)$$

where

$[e]$, $[e]_0$, $[w]$ are respectively the concentration in esters, esters at the initial state and water in mol/L,

$[ac]$ the concentration in carboxylic acid during hydrolysis in mol/L

The concentration in esters has the following analytical solution [41]

$$[e] = [e]_0 \frac{(1+A)\ exp(-Kt)}{1 + A\ \exp(-Kt)} \quad (9)$$

with:

$$K = k_c[e]_f[w] \quad (10)$$

$$[e]_f = [e]_0 + \frac{k_u}{k_c} \quad (11)$$

$$A = \frac{k_c\ [e]_0}{k_u} \quad (12)$$

For next figures and equation, we decided by convenience to use acid functions changes in function of time. Acids can be described as follows:

$$[ac] = [ac]_0 + s = [ac]_0 + [e]_0 - [e]_t \quad (13)$$

$$[ac]_0 = \frac{\rho}{(1-\chi_c)Mn_0} \quad (14)$$

where

ρ is the volumic mass of polymer (in g/L),

M_{n0} the initial number molecular mass of PBT (g/mol) and

χ_c the crystallinity

$$[e]_0 = \frac{2\ \rho}{M_m} \quad (15)$$

with M_m being the monomer molecular mass (g/mol).

This model was first compared to the data published by Goje [40] for the high temperature hydrolysis of PBT. The curves for conversion rate of PBT into its monomers are presented in Fig. 8a. Curves display an auto-accelerated shape in good agreement with Eq. 9. They can be characterized by the values of half time $t_{1/2}$ (i.e. time for consuming half of initially present ester groups) and "induction period" t_i (i.e. the time for "auto-acceleration") which allows to extract A and K values from:

$$t_{1/2} = \frac{\ln(2+A)}{K} \quad (16)$$

$$t_i = \frac{\ln(2+A)}{K} - \frac{2\ (A+1)}{K\ (2+A)} \quad (17)$$

At first, the ability of the model to simulate the sigmoidal shape of PBT hydrolysis curve in the whole range of conversion degree is for us a sufficient argument to validate it. The next step is to identify the rate constants in the whole temperature range.

- at 80°C or 85°C [17], concentration of water is known from DVS study (see 'Results') but exact values of A and K are needed to identify k_u and k_c. However, the degradation curve were here established for the time to embrittlement, i.e. at lower conversion degree than in Fig. 8a, and possible, several k_u, k_c sets could permit an acceptable fit.
- in the conditions studied by Goje, the knowledge of K and A should be sufficient to determine k_u and k_c and later to extrapolate them to other temperatures. However, we lack the concentration of water dissolved in PBT amorphous phase. The water solubility in PBT amorphous phase depends on external pressure (Fig. 1). It must therefore be very high in the conditions investigated by Goje (hydrolysis performed in autoclave under autogenous water pressure). In the absence of relevant data about the temperature effect, the value was considered as constant with temperature.

We thus implemented the following approach:

- results of Fig. 8a were tentatively simulated with several k_u, k_c sets corresponding to several possible water concentrations,
- hydrolysis results at 80°C was simulated with the known concentration in water (from Table 2) so as to get k_u and k_c values at 80°C (Fig. 8b). Other data for hydrolysis at 120°C [43] allowed the determination of a (k_u, k_c) pair at 120°C considering that the pressure is roughly equal to atmospheric pressure.

The "best" set of kinetics parameters retained is that of the greater correlation coefficient of Arrhenius law for each constant and concentration in water (Fig. 9 and Table 4). Despite further refinements needed, it can be considered as a first model for PBT hydrolysis.

4.3. Effect of chain ends on hydrolysis rate

To validate this model in each situation, we were interested in simulating the data obtained by Kelleher et al.[17]. This latter has actually compared the hydrolysis rate of several PBT grades differing by their Melt Flow Index, in other words their initial molar mass (or concentration in carboxylic acid groups) and observed an apparent hydrolysis rate depending on the initial melt flow index, i.e. initial molar mass. Since initial number molar mass directly influence the initial carboxylic acid chain ends concentration (see Eq. 14) and thus the auto-acceleration parameter A (see Eqs. 9 and 12), we considered this was a relevant case for testing the model capability to simulate this auto-acceleration phenomenon.

Using data adjusted from Table and Fig. 8, we extracted the two constants k_u and k_c at 85°C. Using $[ac]_0 = 1/M_{n0}$ as boundary conditions, the model allows to fit the Kelleher et al. data (Fig. 10) without any genuine constant (i.e. for example valid only for one PBT grade) which is a supplementary argument in its favor.

These simulations allow us to conclude that the model describes the oxidation of various grades of PBT. The only important parameters seem to be the initial concentration $1/M_{n0}$ which represents the initial concentration in end chains and crystallinity rate since degradation is only observed in the amorphous phase. From an applicative point of view, this indicates that high fluidity grades are well suited for injection process (from a rheological point of view) but might suffer of a weaker hydrolytic stability. The model can also be used for investigating the hydrolytic degradation occurring in "processing conditions" for insufficiently dried PBT materials.

4.4. Effect of pigments

We demonstrated on the previous section that the modelling is working for each PBT grades tested both picked from literature and

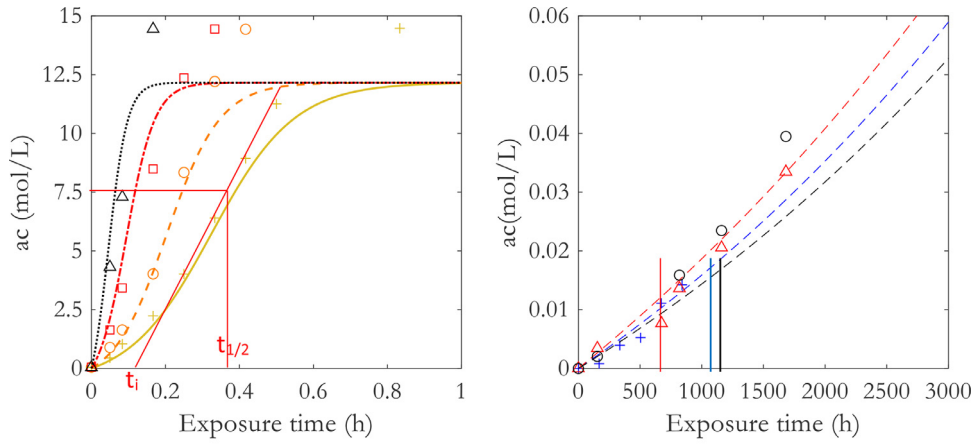

Fig. 8. (a) Kinetic modelling based on Goje's data [40]. Dashed lines represent the modelling, crosses marks represents Goje's data at 200°C (+), 215°C (○), 230°C (□) and 245°C (△). (b) Kinetic modelling based on our study on PBT1 (+), PBT2 (△) and PBT3 (○) at 80C. Dashed lines represent the modelling. Vertical full lines correspond to the embrittlement time for PBT1, PBT2 and PBT3.

Table 4
Rate constants k_u (L/mol/h) and k_c ($L^2/mol^2/h$), w (mol/L) for PBT1, PBT2, PBT3, Goje's [40] and Chisholm's data [43], and activation energy E_a (kJ/mol).

	80°C	85°C	120°C	200°C	215°C	230°C	245°C	E_a	R^2
k_u	8.5×10^{-8}	2.1×10^{-4}	1.3×10^{-5}	5.5×10^{-2}	7.7×10^{-2}	1.7×10^{-1}	3.6×10^{-1}	143	0.997
k_c	3.8×10^{-5}	1.5×10^{-4}	2.9×10^{-5}	9.9×10^{-2}	1.1×10^{-1}	1.8×10^{-1}	1.9×10^{-1}	84	0.985
w	0.44	0.44	0.44	10	10	10	10		

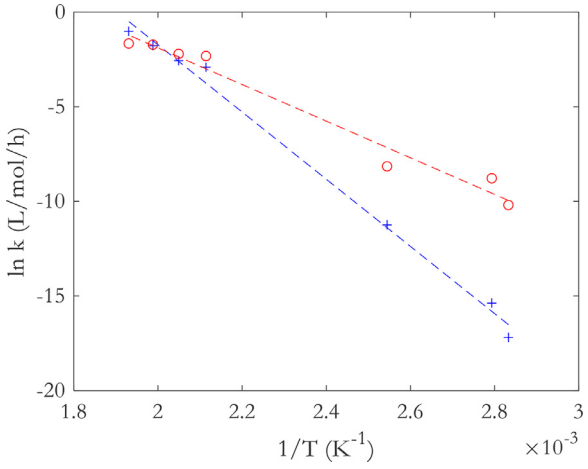

Fig. 9. Arrhenius plot for k_u (+) and k_c (○).

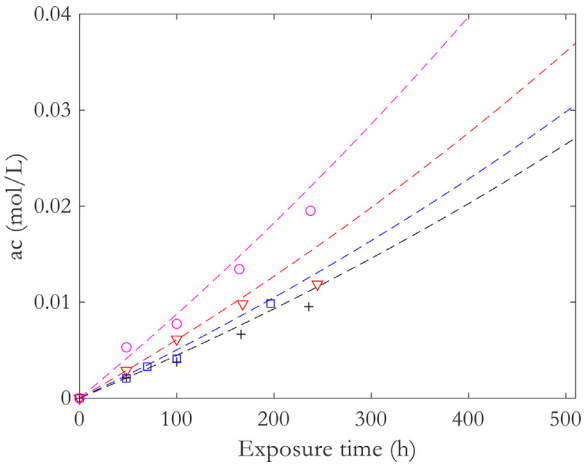

Fig. 10. Kinetic modelling based on Kelleher experimental points MFR4 (+), MFR6 (□), MFR14 (▼) and MFR55 (○).

Table 5
Initial weight molar mass for PBT used in Kelleher et al. study [17].

Labelled	MFR4	MFR6	MFR14	MFR55
Initial M_w (kg/mol)	74.5	65.9	54.1	37.4

the one used for this study. It remains now to discuss and model the clear effect of pigments on hydrolysis rate (Fig. 4b) leading to a faster surface damage (see Supplementary data SI-2). For that purpose, we based on the kinetic model validated at 80°C. To describe pigments effect, we first assumed that water concentration in amorphous phase increased accordingly to DVS data (Fig. 1). The resulting simulations are represented by full lines (Fig. 11) and lead to an underestimation of hydrolysis rate. To better adjust the simulations, we had two possibilities:

① change k_u and k_c, but those kinetic rate constants would be "pigment" dependent, and would not be genuine anymore

② consider that pigments surface chemistry induces a catalytic effect on hydrolysis rate. This can be partially justified by the well-known following facts:

- Carbon black displays a certain acidity [44,45] as illustrated for example by Peña et al. [44,45]
- PBT-G contains copper phthalocyanine. According to visual observations, PBT-G progressively discolors, suggesting that pigment is unstable in presence of water. A possible reaction of

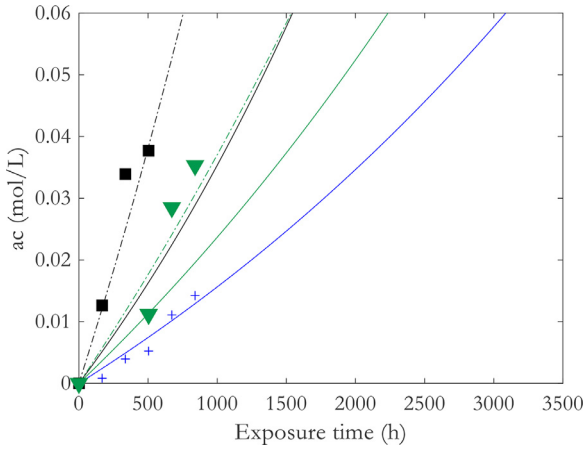

Fig. 11. Chain scission for PBT1 (+) PBT-CB (■), PBT-G (▼) together with kinetic modeling (full and dashed lines – see text).

water with cupric ion would be:

$$Cu^{2+} + 2H_2O \Leftrightarrow Cu(OH)_2 + 2H_3O^+$$

In both cases, hydronium ions would be generated. We hence modified the boundary conditions as follows: $[ac]_0 = 1/M_{n0} + b$ where b results for pigments. Using b = 0.05 mol/L for PBT-G and 0.1 mol/L for PBT-CB, acceptable simulations where obtained (and represented with dashed lines in Fig. 11). It remains however to better model the acid generation in PBT amorphous phase to better justify this new parameter.

5. Conclusions

This paper describes a complete multiscale study of PBT hydrolytic degradation. For summarizing:

- Embrittlement was described in terms of chain scission and chemicrystallization. An Mw - χc map for predicting the embrittlement was completed and militates in favor of an universal embrittlement criterion valid for all PBT grades.
- The hydrolysis kinetics was described by a simple kinetic model taking into account the autocatalysis effect of PBT, due to the presence of carboxylic acids (either initially present chain ends or generated by the hydrolysis reaction). Its kinetic parameters seem to be common to all PBT grades and the only "adjustable" parameters are the initial concentration in chain ends 1/Mn0 and the percentage of absorbed water, both being easily determined for classical physico-chemical tools. This paper also illustrates the effect of the choice of PBT grades on long term hydrolytic stability.
- To our knowledge, the influence of pigments regarding hydrolysis was addressed for the first time. It revealed some interesting phenomena such as higher water uptake and faster hydrolysis kinetics. Futures works should help to link them with possible water clustering at pigments surface and surface reactivity of pigments aggravating the hydrolysis reaction.

Declaration of Competing Interest

We hereby confirm that we have no conflict of interest with the paper

"Multiscale study of poly(butylene terephthalate) hydrolysis" submitted to Polymer Degradation and Stability.

CRediT authorship contribution statement

C. Loyer: Data curation, Formal analysis, Investigation, Writing – original draft, Writing – review & editing. **G. Régnier:** Conceptualization, Funding acquisition, Methodology, Project administration, Supervision, Validation, Writing – original draft. **V. Duval:** Conceptualization, Funding acquisition, Methodology, Project administration, Supervision, Validation, Writing – original draft, Writing – review & editing. **E. Richaud:** Conceptualization, Funding acquisition, Methodology, Project administration, Supervision, Validation, Writing – original draft, Writing – review & editing.

Acknowledgements

The authors would like to thank the ANRT for granting this project (N°2019/1467).

The authors would also like to thank I. Derue for performing DVS experiments and helping in data analysis.

References

[1] B. Fayolle, E. Richaud, X. Colin, J. Verdu, Review: degradation-induced embrittlement in semi-crystalline polymers having their amorphous phase in rubbery state, J. Mater. Sci. 43 (22) (2008) 6999–7012, doi:10.1007/s10853-008-3005-3.
[2] O. Okamba-Diogo, E. Richaud, J. Verdu, F. Fernagut, J. Guilment, B. Fayolle, Investigation of polyamide 11 embrittlement during oxidative degradation, Polymer 82 (2016) 49–56, doi:10.1016/j.polymer.2015.11.025.
[3] A.F. Reano, A. Guinault, E. Richaud, B. Fayolle, Polyethylene loss of ductility during oxidation: effect of initial molar mass distribution, Polym. Degrad. Stab. 149 (2018) 78–84, doi:10.1016/j.polymdegradstab.2018.01.021.
[4] C. Loyer, G. Régnier, V. Duval, Y. Ould, E. Richaud, PBT plasticity loss induced by oxidative and hydrolysis ageing, Polym. Degrad. Stab. 181 (2020) 109368, doi:10.1016/j.polymdegradstab.2020.109368.
[5] N. Manabe, Y. Yokota, The method for analyzing anhydride formed in poly(butylene terephthalate) (PBT) during thermal and photo-degradation processes and applications for evaluation of the extent of degradation, Polym. Degrad. Stab. 69 (2) (2000) 183–190, doi:10.1016/S0141-3910(00)00059-8.
[6] G. Montaudo, C. Puglisi, F. Samperi, Primary thermal degradation mechanisms of Poly(ethylene terephthalate) and Poly(butylene terephthalate), Polym. Degrad. Stab. 42 (1) (1993) 13–28, doi:10.1016/0141-3910(93)90021-A.
[7] F. Samperi, C. Puglisi, R. Alicata, G. Montaudo, Thermal degradation of poly(ethylene terephthalate) at the processing temperature, Polym. Degrad. Stab. 83 (1) (2004) 3–10, doi:10.1016/S0141-3910(03)00166-6.
[8] V. Passalacqua, F. Pilati, V. Zamboni, B. Fortunato, P. Manaresi, Thermal degradation of poly(butylene terephthalate), Polymer 17 (12) (1976) 1044–1048, doi:10.1016/0032-3861(76)90004-5.
[9] S. Carroccio, P. Rizzarelli, G. Scaltro, C. Puglisi, Comparative investigation of photo- and thermal-oxidation processes in poly(butylene terephthalate), Polymer 49 (16) (2008) 3371–3381, doi:10.1016/j.polymer.2008.05.015.
[10] A. Rivaton, Photochemistry of poly(butyleneterephthalate): 2—identification of the IR-absorbing photooxidation products, Polym. Degrad. Stab. 41 (3) (1993) 297–310, doi:10.1016/0141-3910(93)90076-U.
[11] R.J. Gardner, J.R. Martin, Effect of relative humidity on the mechanical properties of poly(1,4-butylene terephthalate), J. Appl. Polym. Sci. 25 (10) (1980) 2353–2361, doi:10.1002/app.1980.070251021.
[12] Z.A.M. Ishak, A. Ari, Effects of hygrothermal aging and a silane coupling agent on the tensile properties of injection molded short glass ®ber reinforced poly(butylene terephthalate) composites, Eur. Polym. J. (2001) 13.
[13] Z.A.M. Ishak, N.C. Lim, Effect of moisture absorption on the tensile properties of short glass fiber reinforced poly(butylene terephthalate), Polym. Eng. Sci. 34 (22) (1994) 1645–1655, doi:10.1002/pen.760342202.
[14] A. Bergeret, L. Ferry, P. Ienny, Influence of the fibre/matrix interface on ageing mechanisms of glass fibre reinforced thermoplastic composites (PA-6,6, PET, PBT) in a hygrothermal environment, Polym. Degrad. Stab. 94 (9) (Sep. 2009) 1315–1324, doi:10.1016/j.polymdegradstab.2009.04.009.
[15] K. Kishore, S. Sankaralingam, Kinetic analysis of the data on the effect of humidity on the stability of poly(butylene terephthalate), Polym. Eng. Sci. 24 (13) (1984) 1043–1046, doi:10.1002/pen.760241308.
[16] A. Bardin, P.-Y.L.e Gac, S. Cérantola, G. Simon, H. Bindi, B. Fayolle, Hydrolytic kinetic model predicting embrittlement in thermoplastic elastomers, Polym. Degrad. Stab. 171 (2020) 109002, doi:10.1016/j.polymdegradstab.2019.109002.
[17] P.G. Kelleher, R.P. Wentz, D.R. Falcone, Hydrolysis of poly(butylene terephthalate), Polym. Eng. Sci. 22 (4) (1982) 260–264, doi:10.1002/pen.760220408.
[18] A. Ballara, J. Verdu, Physical aspects of the hydrolysis of polyethylene terephthalate, Polym. Degrad. Stab. 26 (4) (1989) 361–374, doi:10.1016/0141-3910(89)90114-6.
[19] M.A. Maatoug, et al., Role of pigments in the stability of polyethylene systems, Macromol. Mater. Eng. 282 (2) (2000) 30–36.
[20] R. Az, Pigment decomposition in polymers in applications at elevated temperatures, Dyes Pigm. 15 (1) (1991) 1–14, doi:10.1016/0143-7208(91)87001-4.

[21] P.P. Klemchuk, Influence of pigments on the light stability of polymers: a critical review, Polymer Photochem. 3 (1) (1983) 1–27, doi:10.1016/0144-2880(83)90042-8.

[22] S. Laun, H. Pasch, N. Longiéras, C. Degoulet, Molar mass analysis of polyamides-11 and -12 by size exclusion chromatography in HFiP, Polymer 49 (21) (2008) 4502–4509, doi:10.1016/j.polymer.2008.08.017.

[23] W.W. Yau, J.J. Kirkland, D.D. Bly, Modern Size-Exclusion Liquid Chomatography : Practice f Gel permeation and Ge lfiltration chromatography, First Edition, John Wiley & Sons, Inc., 1979.

[24] K.-H. Illers, Heat of fusion and specific volume of poly(ethylene terephthalate) and "poly(butylene terephthalate)", Colloid Polym. Sci. 258 (2) (1980) 117–124, doi:10.1007/BF01498267.

[25] F. Dubelley, E. Planes, C. Bas, E. Pons, B. Yrieix, L. Flandin, Predictive durability of polyethylene terephthalate toward hydrolysis over large temperature and relative humidity ranges, Polymer 142 (2018) 285–292, doi:10.1016/j.polymer.2018.03.043.

[26] I. Pillin, S. Pimbert, J.-F. Feller, G. Levesque, Crystallization kinetics of poly(butylene terephthalate) (PBT): Influence of additives and free carboxylic acid chain ends, Polym. Eng. Sci. 41 (2) (2001) 178–191, doi:10.1002/pen.10720.

[27] M. Edge, N.S. Allen, R. Gonzalez-Sanchez, C.M. Liauw, S.J. Read, R.B. Whitehouse, The influence of cure and carbon black on the high temperature oxidation of natural rubber I. Correlation of physico-chemical changes, Polym. Degrad. Stab. 64 (2) (1999) 197–205.

[28] J. Schultz, E. Papirer, C. Jacquemart, Mechanism of diffusion of water in carbon black filled polymers, Eur. Polym. J. 22 (6) (1986) 499–503, doi:10.1016/0014-3057(86)90012-1.

[29] J. Crank, G.S. Park, Diffusion in Polymers, Academic Press, London, 1968.

[30] D.W. Van Krevelen, Properties of Polymers, Elsevier, Amsterdam, 1976.

[31] F. Dubelley, E. Planes, C. Bas, E. Pons, B. Yrieix, L. Flandin, Water vapor sorption properties of polyethylene terephthalate over a wide range of humidity and temperature, J. Phys. Chem. B 121 (8) (Mar. 2017) 1953–1962, doi:10.1021/acs.jpcb.6b11700.

[32] A.F. Ghanem, M.A. Yassin, A.M. Rabie, F. Gouanvé, E. Espuche, M.H. Abdel Rehim, Investigation of water sorption, gas barrier and antimicrobial properties of polycaprolactone films contain modified graphene, J. Mater. Sci. (2020), doi:10.1007/s10853-020-05329-4.

[33] L. Smith, V. Schmitz, The effect of water on the glass transition temperature of poly(methyl methacrylate), Polymer 29 (10) (1988) 1871–1878, doi:10.1016/0032-3861(88)90405-3.

[34] M. Arhant, M.L.e Gall, P.-Y.L.e Gac, P. Davies, Impact of hydrolytic degradation on mechanical properties of PET - Towards an understanding of microplastics formation, Polym. Degrad. Stab. 161 (2019) 175–182, doi:10.1016/j.polymdegradstab.2019.01.021.

[35] O. Saito, Effects of high energy radiation on polymers II. End-linking and gel fraction.pdf, J. Phys. Soc. Japan 13 (1958) 1451–1464.

[36] W. McMahon, H.A. Birdsall, G.R. Johnson, C.T. Camilli, Degradation studies of polyethylene terephthalate, J. Chem. Eng. Data 4 (1) (Jan. 1959) 57–79, doi:10.1021/je60001a009.

[37] P. Kiliaris, C.D. Papaspyrides, R. Pfaendner, Influence of accelerated aging on clay-reinforced polyamide 6, Polym. Degrad. Stab. 94 (3) (Mar. 2009) 389–396, doi:10.1016/j.polymdegradstab.2008.11.016.

[38] B. Jacques, M. Werth, I. Merdas, F. Thominette, J. Verdu, Hydrolytic ageing of polyamide 11. 1. Hydrolysis kinetics in water, Polymer 43 (24) (Nov. 2002) 6439–6447, doi:10.1016/S0032-3861(02)00583-9.

[39] A. Launay, F. Thominette, J. Verdu, Hydrolysis of poly(ethylene terephthalate): a kinetic study, Polym. Degrad. Stab. 46 (3) (1994) 319–324, doi:10.1016/0141-3910(94)90148-1.

[40] A.S. Goje, Auto-catalyzed hydrolytic depolymerization of poly(butylene terephthalate) waste at high temperature, Polym.-Plastics Technol. Eng. 45 (2) (2006) 171–181, doi:10.1080/03602550500374012.

[41] E. Richaud, P. Gilormini, M. Coquillat, J. Verdu, Crosslink density changes during the hydrolysis of tridimensional polyesters: crosslink density changes during hydrolysis, Macromol. Theory Simul. 23 (5) (2014) 320–330, doi:10.1002/mats.201300143.

[42] R.C. Golike, S.W. Lasoski, Kinetics of hydrolysis of polyethylene terephthalate films, J. Phys. Chem. 64 (7) (1960) 895–898, doi:10.1021/j100836a018.

[43] B.J. Chisholm, L. Sisti, S. Soloveichik, G. Gillette, Hydrolytic stability of sulfonated poly(butylene terephthalate), Polymer 44 (6) (2003) 1903–1910, doi:10.1016/S0032-3861(02)00932-1.

[44] J. Peña, Factors affecting the adsorption of fatty acids, alcohols and aromatic compounds on to carbon black pigments (flow micro-calorimetry studies), Dyes Pigm. 49 (1) (2001) 29–49, doi:10.1016/S0143-7208(01)00004-3.

[45] J.M. Peña, N.S. Allen, M. Edge, C.M. Liauw, B. Valange, Factors affecting the adsorption of stabilisers on to carbon black (flow micro-calorimetry studies) 4. Secondary antioxidants, Polym. Degrad. Stab. 72 (1) (2001) 31–45, doi:10.1016/S0141-3910(00)00199-3.